

Drops climbing uphill on an oscillating substrate

E. S. BENILOV¹† AND J. BILLINGHAM²

¹Department of Mathematics, University of Limerick, Ireland

²School of Mathematical Sciences, University of Nottingham, University Park,
Nottingham NG7 2RD, UK

(Received 12 June 2010; revised 29 October 2010; accepted 15 December 2010;
first published online 7 March 2011)

Recent experiments by Brunet, Eggers & Deegan (*Phys. Rev. Lett.*, vol. 99, 2007, p. 144501 and *Eur. Phys. J.*, vol. 166, 2009, p. 11) have demonstrated that drops of liquid placed on an inclined plane oscillating vertically are able to climb uphill. In the present paper, we show that a two-dimensional shallow-water model incorporating surface tension and inertia can reproduce qualitatively the main features of these experiments. We find that the motion of the drop is controlled by the interaction of a ‘swaying’ (odd) mode driven by the in-plane acceleration and a ‘spreading’ (even) mode driven by the cross-plane acceleration. Both modes need to be present to make the drop climb uphill, and the effect is strongest when they are in phase with each other.

Key words: capillary flows, drops, thin films

1. Introduction

A liquid drop on a stationary, inclined plane either slides downhill or remains stationary (the latter occurs only if there is sufficient contact-angle hysteresis, i.e. difference between the advancing and receding contact angles). One’s intuition suggests that if the plane is vibrated, a sliding drop continues to slide and a stationary drop either remains stationary (if the vibration is not strong enough) or starts to slide. Recent experiments of Brunet, Eggers & Deegan (2007, 2009), however, showed that drops placed on an inclined plate oscillating vertically can actually climb uphill. This paradoxical result was extended by Noblin, Kofman & Celestini (2009), who experimented with drops on a horizontal substrate oscillating both vertically and horizontally and demonstrated that the mean velocity of the drop can be ‘tuned’ to a given value by varying the phase shift between the two components of the oscillations.

There have been two relevant theoretical studies of drops on vibrating substrates. Daniel, Chaudhury & de Gennes (2005) examined the dynamics of a drop on a horizontal plate vibrating tangentially. Approximating the drop by a forced linear oscillator with a frequency equal to that of the drop’s free oscillations, they showed that the direction of its drift is determined by the anharmonic component of the vibration. A similar conclusion was obtained by Benilov (2010) for drops on an inclined plate oscillating vertically, on the basis of a quasi-static approximation (which assumes that the oscillations are slow, so the drop’s shape is determined by the balance of surface tension, gravity and inertial force). It was shown that the drop can climb uphill provided the time dependence of the plate’s acceleration involves

† Email address for correspondence: eugene.benilov@ul.ie

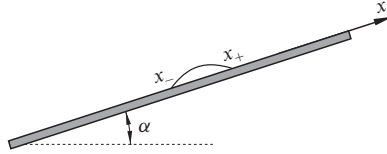


FIGURE 1. The setting: a droplet on an inclined substrate oscillating vertically.

narrow/deep ‘troughs’ and wide/low ‘crests’. Note, however, that the oscillations in the experiments of Brunet *et al.* (2007, 2009) and Noblin *et al.* (2009) were harmonic, i.e. with symmetric crests and troughs – hence, the models of Daniel *et al.* (2005) and Benilov (2010) are not applicable to these cases. One may also mention the paper by Hocking & Davis (2002) who examined a drop on a horizontal plate undergoing tangential harmonic vibration (in which case the drop spreads out without changing its position).

The present work examines the dynamics of a drop on an inclined plate vibrating vertically. As in the experiments by Brunet *et al.* (2007, 2009), we assume the vibration to be sinusoidal. We shall not, however, target quantitative agreement with the experimental results but rather concentrate on the problem’s qualitative aspects. Accordingly, the simplest model will be employed, with two spatial dimensions and *thin* drops (i.e. such that their depths are much smaller than their widths). The quasi-static approximation, however, will not be used, as it neglects the liquid’s inertia, which is one of the crucial factors contributing to the drop’s uphill motion.

This paper has the following structure: in §2, we shall set up the boundary-value problem based on the above assumptions. The limit of weak vibration will be examined asymptotically in §3. The general case will be examined numerically in §4.

2. Formulation of the problem

2.1. The governing equations

Consider a two-dimensional drop of liquid (of density ρ and surface tension σ) on a vertically vibrating plate inclined at an angle α to the horizontal (see figure 1). We shall assume that the Reynolds number is large (as it indeed was in the experiments of Brunet *et al.* 2007, 2009) so that viscous stresses can be neglected; we shall also assume the drop to be thin.

Then, with the coordinate axis x directed along the plate, the governing equations are

$$\frac{\partial u}{\partial t} + u \frac{\partial u}{\partial x} - \frac{\sigma}{\rho} \frac{\partial^3 h}{\partial x^3} + a \cos \alpha \frac{\partial h}{\partial x} + a \sin \alpha = 0, \quad (2.1)$$

$$\frac{\partial h}{\partial t} + \frac{\partial (uh)}{\partial x} = 0, \quad (2.2)$$

where $h(x, t)$ is the lateral thickness of the drop, $u(x, t)$ is the liquid velocity and $a(t)$ is the acceleration due to both gravity and the vibration-induced inertial force (the latter depends on time t). Equations (2.1)–(2.2) constitute the standard shallow-water model with surface tension, which is valid provided the slope of the liquid’s surface is small. Note also that the term involving σ represents the effect of surface tension, and the following two terms represent the hydrostatic pressure gradient due to the variations of the drop’s thickness and the acceleration down the slope.

The contact lines are at $x = x_{\pm}(t)$ (see figure 1). The thickness of the drop vanishes there, and the velocities of the liquid particles at the contact lines must equal the velocities of the contact lines themselves, which gives the boundary conditions

$$h = 0, \quad u = \frac{dx_{\pm}}{dt} \quad \text{at} \quad x = x_{\pm}(t). \quad (2.3)$$

We also assume that the velocities of the contact lines are determined by the contact angles θ_{\pm} , so that

$$\frac{dx_{\pm}}{dt} = \pm v(\theta_{\pm}), \quad \text{where} \quad \theta_{\pm} = \mp \left(\frac{\partial h}{\partial x} \right)_{x=x_{\pm}}. \quad (2.4)$$

Following numerous other researchers (e.g. Hocking 1987; Davis 2002), we shall assume $v(\theta)$ to be a known function such that

$$\left. \begin{aligned} v < 0 & \quad \text{if} \quad \theta < \theta_r, \\ v = 0 & \quad \text{if} \quad \theta_r \leq \theta \leq \theta_a, \\ v > 0 & \quad \text{if} \quad \theta > \theta_a, \end{aligned} \right\} \quad (2.5)$$

where θ_r and θ_a are the boundaries of the *hysteresis interval* (the receding and advancing contact angles, respectively). In the analytical part of this work, we shall assume that the hysteresis interval is of zero length, i.e. $\theta_r = \theta_a = \theta_0$, where θ_0 is the equilibrium contact angle. Even though this model does not allow drops to be static on a motionless inclined substrate (which should be viewed as a shortcoming), its simplicity allows one to explore the qualitative aspects of vibration.

Generally, if $v(\theta)$ is of the form (2.5), it can be shown (see Appendix A) that energy is dissipated (not generated) at the contact lines. Thus, the boundary condition (2.4) models the contact-line friction.

To understand which parameter controls this effect, consider the simplest contact-line law, $v = v'(\theta - \theta_0)$, where v' is a constant. If $v' \rightarrow \infty$, it follows from the boundary condition (2.4) that $\theta \rightarrow \theta_0$ (otherwise, the velocity of the contact line becomes infinite). Hence, the limit $v' \rightarrow \infty$ amounts to the approximation of fixed contact angle – which, as shown in Appendix A, conserves energy. Interestingly, the opposite limit, $v' \rightarrow 0$, also conserves energy: in this case, contact lines do not move at all – hence, there is no dissipation.

We conclude that the strength of the contact-line friction is controlled by the steepness of the contact-line law: if the derivative of $v(\theta)$ is either large or small, the friction is weak – and it is strong for intermediate values of v' .

2.2. Non-dimensionalization

We will use the dimensionless variables

$$u_{nd} = \frac{u}{U}, \quad h_{nd} = \frac{h}{H}, \quad x_{\pm nd} = \frac{x_{\pm}}{X}, \quad x_{nd} = \frac{x}{X}, \quad t_{nd} = \frac{t}{T}, \quad (2.6)$$

$$\theta_{nd} = \frac{X\theta}{H}, \quad a_{nd} = \frac{a}{A}, \quad v_{nd} = \frac{Tv}{X}, \quad (2.7)$$

where the capital letters denote the scales of the corresponding lowercase variables. Surface tension must be a leading-order effect, so we balance it with the material derivative in (2.1) to obtain the velocity and time scales

$$U = \left(\frac{\sigma H}{\rho X^2} \right)^{1/2}, \quad T = \frac{X}{U}. \quad (2.8)$$

If there is no hysteresis, we assume that the length scales are connected by

$$H = \theta_0 X. \quad (2.9)$$

If there is a contact-line hysteresis interval, we use $\theta_0 = (\theta_r + \theta_a)/2$ in (2.9).

Finally, observe that the law of mass conservation implies that the area of the drop is constant. If we denote this area by C and consider it as given by the initial conditions, we can fix the x -lengthscale, X , by requiring that the dimensionless area is $2/3$, which gives, together with (2.9),

$$C = \frac{2}{3}HX \implies X = \sqrt{\frac{3C}{2\theta_0}}. \quad (2.10)$$

In what follows, this normalization will turn out to be convenient.

In terms of the dimensionless variables (2.6)–(2.10), the governing equations (2.1)–(2.4) become (with subscript nd omitted)

$$\frac{\partial u}{\partial t} + u \frac{\partial u}{\partial x} - \frac{\partial^3 h}{\partial x^3} = -\varepsilon a \left(1 + \gamma \frac{\partial h}{\partial x} \right), \quad (2.11)$$

$$\frac{\partial h}{\partial t} + \frac{\partial(uh)}{\partial x} = 0, \quad (2.12)$$

$$h = 0, \quad u = \frac{dx_{\pm}}{dt} \quad \text{at} \quad x = x_{\pm}, \quad (2.13)$$

$$\frac{dx_{\pm}}{dt} = \pm v(\theta_{\pm}), \quad \text{where} \quad \theta_{\pm} = \mp \left(\frac{\partial h}{\partial x} \right)_{x=x_{\pm}}, \quad (2.14)$$

where

$$\varepsilon = \frac{AT \sin \alpha}{U}, \quad \gamma = \frac{\theta_0}{\tan \alpha}, \quad (2.15)$$

and T , U , H and X are determined by (2.8)–(2.10).

Parameters ε and γ are the main dimensionless parameters of the problem: the former characterizes the strength of the substrate's acceleration and gravity relative to surface tension and inertia, and the latter measures the hydrostatic pressure gradient relative to the acceleration down the slope.

3. The limit of small acceleration

In this section, we study the asymptotic solution when the acceleration is small, $\varepsilon \ll 1$. Note that, even though ε was not small in the experiments of Brunet *et al.* (2007, 2009), the asymptotic results will allow us to elucidate the essential mechanism of the effect. Then, in §4, we shall see that the basic conclusions reached for $\varepsilon \ll 1$ will allow us to interpret the dynamics for $\varepsilon = O(1)$.

We shall also assume that gravity is much weaker than the inertial force due to the substrate's oscillations $A \gg g$, as was the case in the experiments of Brunet *et al.* (2007, 2009). Accordingly, we set

$$a = \sin \omega t + \varepsilon g_{nd}, \quad (3.1)$$

where

$$g_{nd} = \frac{g}{A\varepsilon} \quad (3.2)$$

is the dimensionless acceleration due to gravity (we drop the subscript nd in what follows).

In this section, we assume that the relationship between the contact-line velocity v and the contact angle θ does not involve a hysteresis interval and has Taylor series expansion

$$v(\theta) = v'(\theta - 1) + \frac{v''}{2}(\theta - 1)^2 + \frac{v'''}{6}(\theta - 1)^3 + \dots, \quad (3.3)$$

where v' , v'' , \dots are the derivatives of $v(\theta)$ at $\theta = 1$ (recall that the problem was non-dimensionalized in such a way that $\theta = 1$ at equilibrium, implying $v(1) = 0$).

We shall start by introducing the half-width of the drop and the velocity of its centre:

$$D(t) = \frac{1}{2}(x_+ - x_-), \quad V(t) = \frac{1}{2}\left(\frac{dx_+}{dt} + \frac{dx_-}{dt}\right). \quad (3.4)$$

It is convenient to change to the co-moving reference frame associated with the centre of the drop, and subtract V from the liquid velocity u , which corresponds to the change of variables

$$x_{new} = x - \frac{1}{2}(x_+ + x_-), \quad t_{new} = t, \quad (3.5)$$

$$u_{new} = u - V, \quad h_{new} = h. \quad (3.6)$$

Substituting (3.3)–(3.5) into (2.11)–(2.14), (3.1) and omitting the subscript new , we obtain

$$\frac{\partial u}{\partial t} + \frac{dV}{dt} + u\frac{\partial u}{\partial x} - \frac{\partial^3 h}{\partial x^3} = -\varepsilon(\sin \omega t + \varepsilon g) \left(1 + \gamma \frac{\partial h}{\partial x}\right), \quad (3.7)$$

$$\frac{\partial h}{\partial t} + \frac{\partial(uh)}{\partial x} = 0, \quad (3.8)$$

$$h = 0, \quad u = \pm \frac{dD}{dt} \quad \text{at} \quad x = \pm D, \quad (3.9)$$

$$V \pm \frac{dD}{dt} = \pm v(\theta_{\pm}), \quad (3.10)$$

where

$$\theta_{\pm} = \mp \left(\frac{\partial h}{\partial x}\right)_{x=\pm D}. \quad (3.11)$$

We now seek a solution of the form

$$u = \varepsilon u^{(1)} + \varepsilon^2 u^{(2)} + \dots, \quad h = h^{(0)} + \varepsilon h^{(1)} + \varepsilon^2 h^{(2)} + \dots, \quad (3.12)$$

$$V = \varepsilon V^{(1)} + \varepsilon^2 V^{(2)} + \dots, \quad D = D^{(0)} + \varepsilon D^{(1)} + \varepsilon^2 D^{(2)} + \dots. \quad (3.13)$$

The zeroth-order solution is the unperturbed stationary drop:

$$D^{(0)} = 1, \quad h^{(0)} = \frac{1}{2}(1 - x^2). \quad (3.14)$$

Observe that the dimensionless area of the drop determined by (3.14) indeed equals $2/3$, as required by our non-dimensionalization (see (2.10)). It also implies that all higher order corrections have zero net volume.

In what follows, we show that the mean velocity of the drop is proportional to ε^2 . Thus, we need to explore the first and second orders of the expansion in ε , which will be done in §§3.1 and 3.2. Then, in §3.3, we will discuss the physical meaning of the results.

3.1. The first-order solution

At $O(\varepsilon)$, the governing equations (3.7)–(3.10) yield

$$\frac{\partial u^{(1)}}{\partial t} + \frac{dV^{(1)}}{dt} - \frac{\partial^3 h^{(1)}}{\partial x^3} = - \left(1 + \gamma \frac{\partial h^{(0)}}{\partial x} \right) \sin \omega t, \quad (3.15)$$

$$\frac{\partial h^{(1)}}{\partial t} + \frac{\partial(u^{(1)}h^{(0)})}{\partial x} = 0, \quad (3.16)$$

$$h^{(1)} \pm \frac{\partial h^{(0)}}{\partial x} D^{(1)} = 0, \quad u^{(1)} = \pm \frac{dD^{(1)}}{dt} \quad \text{at } x = \pm D^{(0)}, \quad (3.17)$$

$$V^{(1)} \pm \frac{dD^{(1)}}{dt} = -v' \left(\frac{\partial h^{(1)}}{\partial x} \pm \frac{\partial^2 h^{(0)}}{\partial x^2} D^{(1)} \right)_{x=\pm D^{(0)}}. \quad (3.18)$$

These equations describe small oscillations of the drop, forced by the vibration of the substrate.

Clearly, the drop can experience a sustained uphill motion only if the corresponding solution is periodic in t . Given that our problem is dissipative and, thus, the drop does not have neutrally stable ‘natural’ frequencies, any periodic solution must have the period of the forcing. Furthermore, since (3.15)–(3.18) are linear, their solution should be harmonic with a single frequency ω (as opposed to a *nonlinear* oscillatory system, whose response to a harmonic forcing of frequency ω would involve frequencies ω , 2ω , 3ω , etc.).

Accordingly, we shall seek a solution of (3.15)–(3.18) in the form

$$u^{(1)}(x, t) = \text{Re} [u_1^{(1)}(x) e^{i\omega t}], \quad h^{(1)}(x, t) = \text{Im} [h_1^{(1)}(x) e^{i\omega t}], \quad (3.19)$$

$$V^{(1)}(t) = \text{Re} (V_1^{(1)} e^{i\omega t}), \quad D^{(1)}(t) = \text{Im} (D_1^{(1)} e^{i\omega t}), \quad (3.20)$$

where $u_1^{(1)}$, $h_1^{(1)}$, $V_1^{(1)}$ and $D_1^{(1)}$ are the new unknowns. Substituting (3.19)–(3.20) into (3.15)–(3.18) and taking into account that the leading-order solution is given by (3.14), we obtain

$$\omega u_1^{(1)} + \omega V_1^{(1)} + \frac{d^3 h_1^{(1)}}{dx^3} = 1 - \gamma x, \quad \omega h_1^{(1)} + \frac{1}{2} \frac{d[u_1^{(1)}(1-x^2)]}{dx} = 0, \quad (3.21)$$

$$h_1^{(1)} = D_1^{(1)}, \quad u_1^{(1)} = \pm \omega D_1^{(1)} \quad \text{at } x = \pm 1, \quad (3.22)$$

$$\frac{dh_1^{(1)}}{dx} = \frac{1}{iv'} (V_1^{(1)} \pm \omega D_1^{(1)}) \pm D_1^{(1)} \quad \text{at } x = \pm 1. \quad (3.23)$$

It is instructive to separate the even and odd parts of the solution:

$$h_1^{(1)} = h_{1e}^{(1)} + h_{1o}^{(1)}, \quad (3.24)$$

where

$$h_{1e}^{(1)}(-x) = h_{1e}^{(1)}(x), \quad h_{1o}^{(1)}(-x) = -h_{1o}^{(1)}(x). \quad (3.25)$$

Then, (3.21)–(3.23) splits into two boundary-value problems, each set on half of the original interval, say $(-1, 0)$,

$$\omega u_{1e}^{(1)} + \omega V_1^{(1)} + \frac{d^3 h_{1o}^{(1)}}{dx^3} = 1, \quad \omega h_{1o}^{(1)} + \frac{1}{2} \frac{d[u_{1e}^{(1)}(1-x^2)]}{dx} = 0, \quad (3.26)$$

$$h_{1o}^{(1)} = 0, \quad u_{1e}^{(1)} = 0, \quad \frac{dh_{1o}^{(1)}}{dx} = \frac{1}{iv'} V_1^{(1)} \quad \text{at } x = -1, \quad (3.27)$$

$$\frac{du_{1e}^{(1)}}{dx} = 0, \quad \frac{d^2 h_{1o}^{(1)}}{dx^2} = 0 \quad \text{at } x = 0, \quad (3.28)$$

and

$$\omega u_{1o}^{(1)} + \frac{d^3 h_{1e}^{(1)}}{dx^3} = -\gamma x, \quad \omega h_{1e}^{(1)} + \frac{1}{2} \frac{d[u_{1o}^{(1)}(1-x^2)]}{dx} = 0, \quad (3.29)$$

$$h_{1e}^{(1)} = D_1^{(1)}, \quad u_{1o}^{(1)} = -\omega D_1^{(1)}, \quad \frac{dh_{1e}^{(1)}}{dx} = -\left(\frac{\omega}{iv'} + 1\right) D_1^{(1)} \quad \text{at } x = -1, \quad (3.30)$$

$$u_{1o}^{(1)} = 0, \quad \frac{dh_{1e}^{(1)}}{dx} = 0 \quad \text{at } x = 0. \quad (3.31)$$

The boundary-value problem (3.26)–(3.28) describes *anti-symmetric* variations $h_{1o}^{(1)}$ of the drop's shape, so that the drop sways from side to side (the *swaying mode*). Note that $D_1^{(1)}$ does not appear in (3.26)–(3.28), i.e. variations of the drop's width do not affect the swaying mode.

Problem (3.29)–(3.31), in turn, describes *symmetric* variations of the drop's shape and width (the *spreading mode*). Note that (3.29)–(3.31) are independent of $V_1^{(1)}$ – thus, the drop's velocity is unimportant in this case. Generally, however, both modes are present in the solution, although $D_1^{(1)}$ or $V_1^{(1)}$ can occasionally vanish for a particular set of the parameters involved.

We can also identify the physical mechanisms generating the swaying and spreading modes. To do so, one needs to trace the forcing terms in the respective boundary-value problems back to the original equations (2.11)–(2.14) (the physical meaning of which is well known). The $-\gamma x$ term in the first equation of (3.29) and the unity in the first equation of (3.26) originate from the two terms on the right-hand side of (2.11). We conclude that the spreading mode is generated by the alternating hydrostatic pressure gradient, whereas the swaying mode is generated by the alternating acceleration down the slope.

Further properties of the first-order boundary-value problem (3.21)–(3.23), as well as a numerical method for solving it, are discussed in Appendix B.

3.2. The second-order solution

There are two ways of obtaining the second-order solution. The straightforward one is to expand the exact equations (3.7)–(3.10) up to the second order and solve them. It can be anticipated that the second-order solution describes a superposition of a time-independent part and oscillations of frequency 2ω . The second-order velocity $V^{(2)}$, for example, should have the form

$$V^{(2)} = V_0^{(2)} + \text{Re} \left(V_2^{(2)} e^{2i\omega t} \right). \quad (3.32)$$

The first term in this expression is the drop's mean drift velocity, which we are mainly interested in. This approach, however, involves a lot of cumbersome algebra and, thus, is included in Appendix D – whereas, in the main body of the paper, a simpler,

less formal approach is presented, based on conservation laws. It does not allow one to find the full solution, but still provides a means for calculating its most important part, the mean velocity $V_0^{(2)}$.

Recall that our equations were non-dimensionalized in such a way that the dimensionless area of the drop is

$$\int_{-D}^D h \, dx = \frac{2}{3}. \quad (3.33)$$

Next, a momentum balance equation can be derived from the governing set (3.7)–(3.10), taking into account (3.33), in the form

$$\frac{d}{dt} \left(\int_{-D}^D hu \, dx + \frac{2}{3}V \right) + \left[\frac{1}{2} \left(\frac{\partial h}{\partial x} \right)^2 \right]_{x=D} - \left[\frac{1}{2} \left(\frac{\partial h}{\partial x} \right)^2 \right]_{x=-D} = -\frac{2}{3}\varepsilon(\sin \omega t + \varepsilon g). \quad (3.34)$$

Recalling that we are interested in solutions that are periodic with period

$$P = \frac{2\pi}{\omega}, \quad (3.35)$$

we integrate (3.34) from $t=0$ to $t=P$, which yields

$$\left[\overline{\left(\frac{\partial h}{\partial x} \right)^2} \right]_{x=D} - \left[\overline{\left(\frac{\partial h}{\partial x} \right)^2} \right]_{x=-D} = -\frac{4}{3}\varepsilon^2 g, \quad (3.36)$$

where the bar denotes averaging over the period. Note that (3.36) is exact.

To further simplify (3.36), we relate the contact angle to the contact-line velocity, i.e. ‘invert’ the original boundary condition (3.10) by rewriting it in the form

$$\left(\frac{\partial h}{\partial x} \right)_{x=\pm D} = \mp \theta(v_{\pm}), \quad (3.37)$$

where

$$v_{\pm} = \pm V + \frac{dD}{dt}. \quad (3.38)$$

Here, $\theta(v)$ is the inverse function to $v(\theta)$, and v_{\pm} are the velocities of the contact lines (their signs are chosen in such a way that, for an advancing contact line, $v_{\pm} > 0$). Note that the first-order results imply

$$V = O(\varepsilon), \quad \frac{dD}{dt} = O(\varepsilon); \quad (3.39)$$

hence, $|v_{\pm}| \ll 1$. Accordingly, one can ‘invert’ expression (3.3) for the contact-line velocity in the form of a series in the powers of v and, thus, obtain

$$\theta = 1 + \frac{v}{v'} - \frac{v''}{2(v')^3} v^2 + O(v^3), \quad (3.40)$$

after which (3.37) becomes

$$\left(\frac{\partial h}{\partial x} \right)_{x=\pm D} = \mp \left[1 + \frac{1}{v'} \left(\pm V + \frac{dD}{dt} \right) - \frac{v''}{2(v')^3} \left(\pm V + \frac{dD}{dt} \right)^2 + O(\varepsilon^3) \right]. \quad (3.41)$$

Substituting this expression into (3.36) and taking into account (3.39), we obtain

$$\bar{V} = \frac{1}{v'} \left(\frac{v''}{v'} - 1 \right) \overline{V \frac{dD}{dt}} - \frac{1}{2} \varepsilon^2 v' g + O(\varepsilon^3). \quad (3.42)$$

Finally, it follows from the first-order solution (3.20) that

$$V = \frac{1}{2} \varepsilon (V_1^{(1)} e^{i\omega t} + V_1^{(1)*} e^{-i\omega t}) + O(\varepsilon^2), \quad \frac{dD}{dt} = \frac{1}{2} i \varepsilon \omega (D_1^{(1)} e^{i\omega t} + D_1^{(1)*} e^{-i\omega t}) + O(\varepsilon^2), \quad (3.43)$$

after which (3.42) yields

$$\bar{V} \approx \varepsilon^2 \left[\frac{\omega}{2v'} \left(\frac{v''}{v'} - 1 \right) \operatorname{Re} (V_1^{(1)} D_1^{(1)*}) - \frac{v' g}{2} \right]. \quad (3.44)$$

This is the final product of our derivation and relates the mean velocity of the drop to the first-order solution $V_1^{(1)}$ and $D_1^{(1)}$, determined by the boundary-value problem (3.21)–(3.23).

3.3. Discussion

(i) The two terms in expression (3.44) for \bar{V} represent the effects of the substrate's oscillation and gravity. Observe that the former is non-zero only if both $V_1^{(1)}$ and $D_1^{(1)}$ are non-zero – thus, to make the drop move, both the swaying and spreading modes must be present. At the same time, non-zero $V_1^{(1)}$ and $D_1^{(1)}$ do not guarantee that the vibration necessarily makes the drop drift up or down the slope, since the first term of (3.44) vanishes if the product $V_1^{(1)} D_1^{(1)*}$ is purely imaginary, i.e. if the phase difference between the swaying and spreading modes is $\pm\pi/2$.

(ii) Observe that (3.44) produces a non-zero velocity even if $g=0$, which brings up an interesting question: how does a drop on a symmetrically oscillating substrate 'know' which way to go in the absence of gravity? To answer it, observe that, even if $g=0$, the original equations (2.11)–(2.14) are still *not* invariant with respect to the change $x \rightarrow -x$. As a result, the substrate's oscillation generates both even and odd (spreading and swaying) modes, and the specifics of their interaction determine which way the drop moves.

(iii) Observe also that the contribution of gravity to the mean velocity is always negative (as it should be), whereas the first term in expression (3.44) is either negative or positive. To determine its sign, \bar{V} was computed (by numerical integration of the boundary-value problem (3.21)–(3.23)) for $g=0$ and various values of the other parameters involved.

Typical examples of the dependence \bar{V} on ω are shown in figure 2, and two characteristic features can be observed. Firstly, the peak value of \bar{V} in (a) exceeds noticeably that in (b). Secondly, (a) and (b) differ in how $\bar{V}(\omega)$ approaches zero as $\omega \rightarrow 0$: in (a) \bar{V} is positive, and in (b) \bar{V} is negative.

The latter feature can be clarified by analysing the problem's low-frequency limit, as presented in Appendix C.1. Assuming for simplicity $g=0$, one can use expression (C 14) to derive a criterion distinguishing the two 'types' of $\bar{V}(\omega)$ shown in figures 2(a) and 2(b),

$$\left(1 - \frac{v''}{v'} \right) \left[1 - \frac{2(v')^2}{3} \right] \geq 0, \quad (3.45)$$

where the '>' corresponds to figure 2(a).

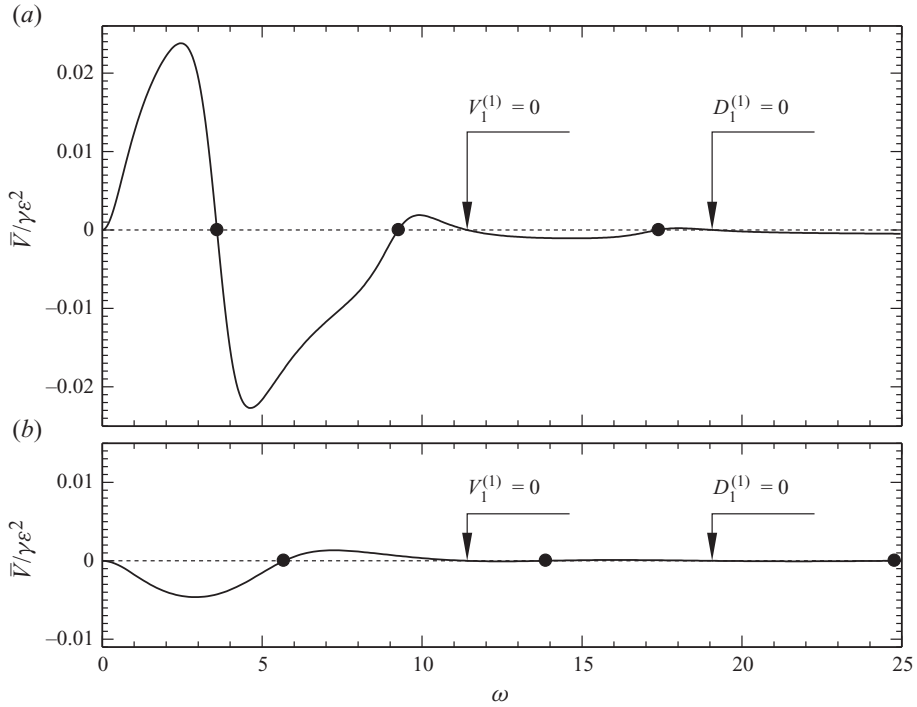


FIGURE 2. The mean velocity, \bar{V} , of the drop versus the frequency ω of the oscillations, as determined by (3.44), for $g=0$, $v''=0$ and (a) $v'=0.5$, (b) $v'=2$. The regions where $\bar{V} > 0$ correspond to the drop climbing uphill. The black dots show the real parts of the drop's 'natural' frequencies; some of the zeros of $\bar{V}(\omega)$ are located very close to these points (such zeros are due to $\text{Re}(V_1^{(1)}D_1^{(1)*})=0$, i.e. the phase difference between the swaying and spreading modes is $\pm\pi/2$). Other zeros of $\bar{V}(\omega)$ are indicated by arrows (these are due to either $V_1^{(1)}=0$ or $D_1^{(1)}=0$, i.e. when one of the two modes of the forced oscillations is absent).

(iv) Our computations showed that the dependence $\bar{V}(\omega)$ is always oscillatory (see the examples in figure 2).

Generally, the oscillatory nature of $\bar{V}(\omega)$ seems to suggest that the observed extrema are caused by a resonance between the forced oscillations and one of the drop's natural frequencies. Note that all of the latter have imaginary parts (due to the dissipation of energy at the contact lines) – hence, the resonance cannot be precise, but it could still strengthen the forced oscillations and, thus, make the drop move faster. We shall see, however, that this hypothesis is incorrect. To test it, we examined the linearized boundary-value problem for free oscillations of a capillary drop (which can be obtained from problem (3.21)–(3.23) for forced oscillations by omitting the forcing term $1 + \gamma x$ from the first equation of (3.21)). The resulting set should be treated as an eigenvalue problem, with ω the eigenvalue. Note that the omission of the (non-symmetric) forcing term makes the free-oscillation problem invariant with respect to the change $x \rightarrow -x$. Accordingly, its eigenfunctions are either even or odd. Physically, this means that a resonance with a natural oscillation can generate either the spreading or swaying mode, but not both together. We solved the eigenvalue problem for free oscillations numerically. Surprisingly, the real parts of the computed eigenvalues do *not* coincide with the extrema of $\bar{V}(\omega)$, but rather with its zeros (see figure 2).

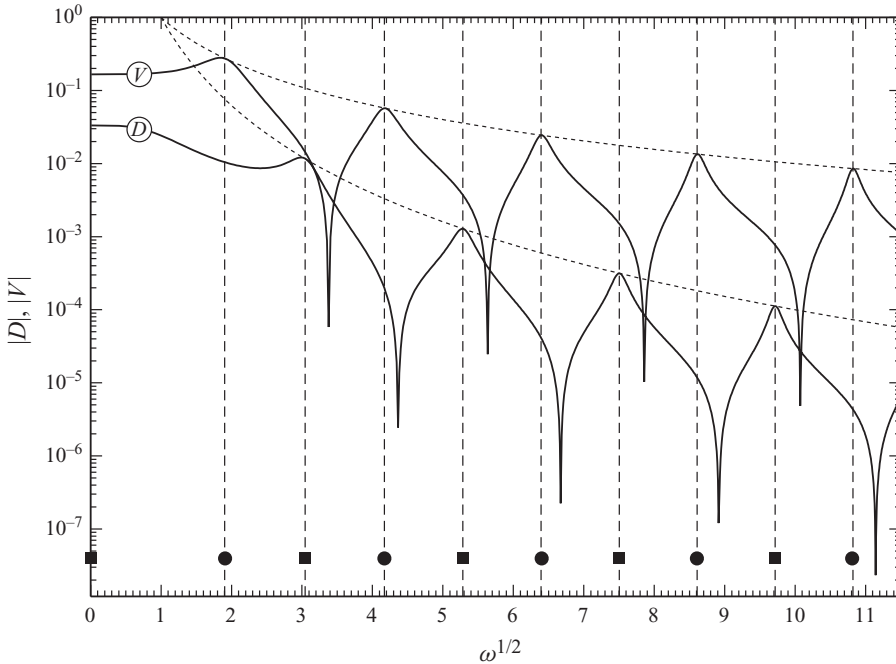


FIGURE 3. The absolute values of V and D as functions of $\omega^{1/2}$, as determined by the boundary-value problem (3.21)–(3.23) with $\gamma=1$ and $v'=0.5$. The vertical dashed lines show the real parts of the natural frequencies of the drop's free oscillations (squares/circles correspond to even/odd modes). The dotted lines show the dependences ω^{-1} and ω^{-2} .

To understand why, we plotted the natural frequencies together with the solutions $V^{(1)}$ and $D^{(1)}$ of the forced problem in figure 3. One can see that the maxima of $|V^{(1)}|$ correspond to resonances with odd natural modes, and the maxima of $|D^{(1)}|$ correspond to resonances with even natural modes. It turns out, however, that the phase difference between $V^{(1)}$ and $D^{(1)}$ at the resonant values of ω is very close to $\pm\pi/2$ (this conclusion was derived from our numerical results, and it was confirmed in the limit $\omega \gg 1$ – see Appendix C.2). As a result, the term $\text{Re}(V^{(1)}D^{(1)})$ in expression (3.44) is negligible, i.e. the forced oscillations do not contribute to the mean velocity \bar{V} .

One has to conclude that there is no direct connection between the natural frequencies of a drop and its motion forced by the substrate's oscillations.

(v) It follows from problem (3.29)–(3.31) for the spreading mode that $D_1^{(1)}$ scales with γ , whereas the ‘swaying problem’ (3.26)–(3.28) is independent of γ , and so is $V_1^{(1)}$. As a result, the effect of the substrate oscillations on the drop (the first term in expression (3.44)) is proportional to γ , and it vanishes if $\gamma=0$.

(vi) It is instructive to consider the limit $v' \rightarrow \infty$ corresponding to a fixed contact angle (and, thus, zero friction between the substrate and contact lines – see Appendix A). In this case, the first term of expression (3.44) vanishes, i.e. the substrate oscillations cannot move the drop – whereas the second (gravity-induced) term of (3.44) tends to infinity. As a result, the drop rapidly slides down.

Neither of the above conclusions should come as a surprise to anybody who has ever tried to climb a slippery slope.

4. Numerical solutions of the full shallow-water equations

We now consider numerical solutions of the boundary-value problem given by (2.11)–(2.14) along with the initial condition

$$h = \frac{1}{2}(1 - x^2), \quad u = 0 \quad \text{at} \quad t = 0. \quad (4.1)$$

4.1. The method

The first step is to reformulate the problem on a fixed domain by defining

$$X = \frac{x - x_+(t)}{W(t)}, \quad (4.2)$$

where

$$W(t) = x_+(t) - x_-(t), \quad (4.3)$$

so that $0 \leq X \leq 1$. The governing equations can then be written in conservative form as

$$\frac{\partial}{\partial t} (Wh) + \frac{\partial}{\partial X} \left[\left(u - \frac{dx_-}{dt} - X \frac{dW}{dt} \right) h \right] = 0, \quad (4.4)$$

$$\frac{\partial}{\partial t} (Wuh) + \frac{\partial}{\partial X} \left[u^2 h + \frac{1}{2} \varepsilon \gamma a h^2 - \left(\frac{dx_-}{dt} + X \frac{dW}{dt} \right) u h \right] = \frac{h}{W^2} \frac{\partial^3 h}{\partial X^3} - \varepsilon a h W, \quad (4.5)$$

which we can display compactly as

$$\frac{\partial \mathbf{Y}}{\partial t} + \frac{\partial \mathbf{F}}{\partial X} = \mathbf{Q}, \quad (4.6)$$

where $\mathbf{Y} = (Wh, WUh)$, and \mathbf{F} and \mathbf{Q} are the fluxes and sources.

Because of the third derivative term in (4.5), this initial value problem is very stiff, so we use a fully implicit central difference method in the form

$$\frac{Y_j^{t+\Delta t} - Y_i^t}{\Delta t} + \frac{F_{j+1}^{t+\Delta t} - F_{j-1}^{t+\Delta t}}{2\Delta x} = Q_i^{t+\Delta t}, \quad (4.7)$$

where j indexes the uniform spatial grid and Δt is the time step. Note that the time step is now constrained by accuracy rather than numerical stability, and we have to solve a system of nonlinear algebraic equations at each time step. We do this using quasi-Newton iteration, calculating the Jacobian using finite differences. Although the most severe computational bottleneck is the calculation of the Jacobian, we find that we are able to reuse the same Jacobian, not just for many iterations, but for many time steps, so that this method is very effective (a typical solution for $0 \leq t \leq 200$ takes a couple of minutes on a dual-core desktop PC).

When ε is moderate to large, we find that a spurious, gridscale oscillation can appear in the solution, even using this fully implicit formulation. This phenomenon has been observed in other simulations of flows dominated by inertia and surface tension (e.g. Dold 1992) and was further investigated in the context of a semi-implicit spectral method by Cenicerros & Hou (1998), where it was shown that filtering of a spurious high-frequency component leads to a stable numerical method. Here, we apply an 11-point smoothing function to u alone every 0.25 time units (Dold 1992), which eliminates this instability without adversely affecting accuracy of the solution (as has been ascertained for the problem at hand by varying the parameters of the filter and the time intervals between its applications).

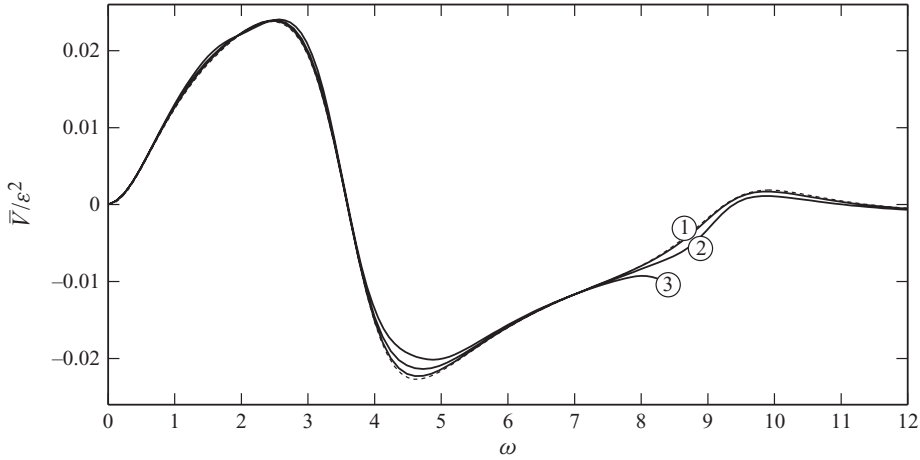


FIGURE 4. The mean velocity \bar{V} versus the frequency ω , as computed through simulations of the exact equations (3.7)–(3.10) for $g=0$, $\gamma=5$, and the linear contact-line law (4.8) with $v'=0.5$. The solid curves correspond to (1) $\varepsilon=0.01$, (2) $\varepsilon=0.25$ and (3) $\varepsilon=0.75$. Curve 3 terminates at $\omega \approx 8.3$ (due to the drop's motion becoming so violent that its free surface touches down on the plate at an interior point). The dotted curve corresponds to the asymptotic (small- ε) limit.

4.2. The results

Figure 4 shows the mean velocity of the drop as a function of ω , for various values of ε and a linear relationship between the contact angle and the contact-line velocity:

$$v(\theta) = v'(\theta - 1). \quad (4.8)$$

The velocity clearly scales with ε^2 even for moderate values of ε , and the agreement between asymptotic and numerical solutions is very good. For larger values of ε , the oscillation of the drop is so violent that the free surface touches down on the plate at some point in the interior (i.e. $h=0$ for some x such that $x_- < x < x_+$), and the simulation cannot proceed further. This corresponds to a breakup of the drop (a three-dimensional equivalent of which has indeed been observed by Brunet *et al.* 2007, 2009).

We have also examined a modified contact-line law

$$v(\theta) = v'(\theta - 1)\theta^{-1/2}, \quad (4.9)$$

so that $v \rightarrow \infty$ as $\theta \rightarrow 0$, making it easier for θ to remain above zero. Note that we do not claim that there is any physical basis for this modified law; we have introduced it to give us some insight into the dynamics of the drop when the amplitude of the motion is not small. Figure 5 shows that the touch-down of the drop's free surface on the plate still occurs in this case, but for slightly larger ε . Observe also that, unlike the previous case of the linear contact-line law (4.8), the small- ε results for (4.9) are no longer valid for order-1 ε . This suggests that the error of our asymptotic results is mainly caused by the drop accessing the nonlinear parts of the contact-line law, whereas the nonlinearity of the governing equations contributes a smaller error. Finally, the mean velocity in case (4.9) is larger than that for (4.8), simply because the contact-line velocity is larger at small contact angles (this effect is particularly strong in the region $9 \lesssim \omega \lesssim 11$, which also seems to be very sensitive to increasing amplitude of the substrate's oscillation).

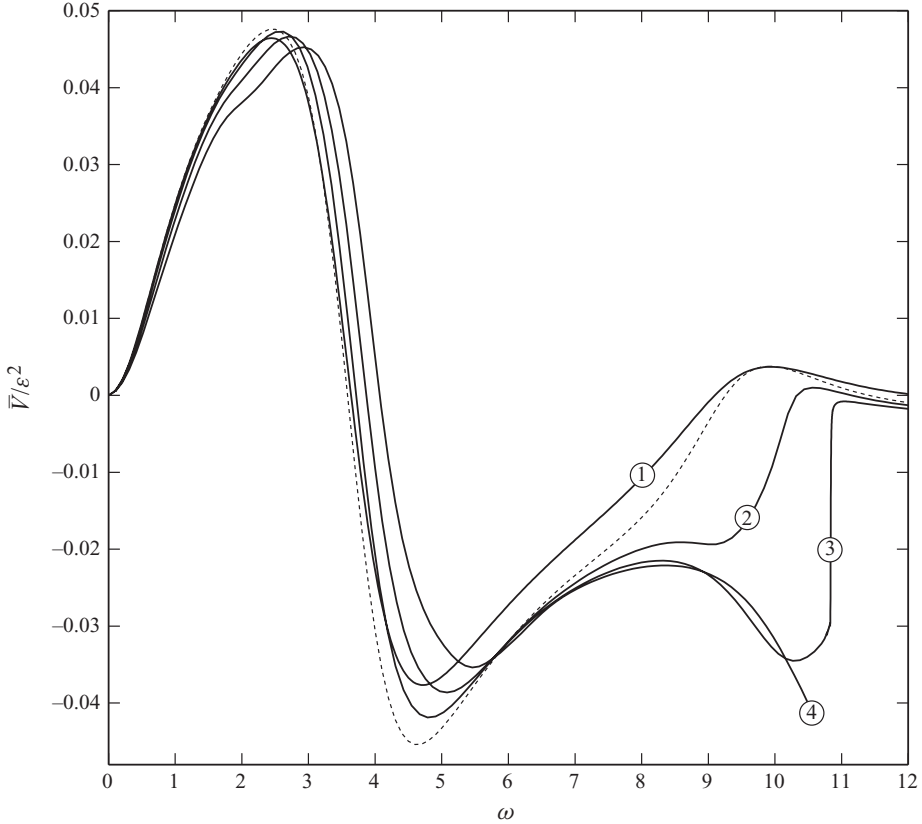


FIGURE 5. As in figure 4, but for the nonlinear contact-line law (4.9) and (1) $\varepsilon=0.25$, (2) $\varepsilon=0.5$, (3) $\varepsilon=0.75$ and (4) $\varepsilon=1$. Curve 4 terminates at $\omega \approx 10.5$ (due to the drop's free surface touching down on the plate at an interior point). The dotted curve corresponds to the asymptotic (small- ε) limit.

To examine the effect of hysteresis, we considered

$$\left. \begin{aligned} v(\theta) &= v' (\theta - \theta_r) \left(\frac{\theta}{\theta_r}\right)^{-1/2} && \text{if } \theta < \theta_r, \\ v(\theta) &= 0 && \text{if } \theta_r \leq \theta \leq \theta_a, \\ v(\theta) &= v' (\theta - \theta_a) \left(\frac{\theta}{\theta_r}\right)^{-1/2} && \text{if } \theta > \theta_a, \end{aligned} \right\} \quad (4.10)$$

and the results are presented in figure 6. As the width of the hysteresis interval increases, maxima of $\bar{V}(\omega)$ appear to shift towards the natural frequencies of the drop's free oscillations. This is probably caused by the fact that, if the hysteresis interval is wide, the contact lines are pinned to the substrate during most of the cycle – unless the drop's oscillations are very strong, of course, which can only be achieved if the forcing frequency is close to one of the drop's natural frequencies.

Figure 7 shows how the shape of the drop varies during one cycle of the oscillation with a frequency near the one giving the maximum rise velocity. Notice how the drop shapes in three out of the eight frames are noticeably sloped upwards, with only

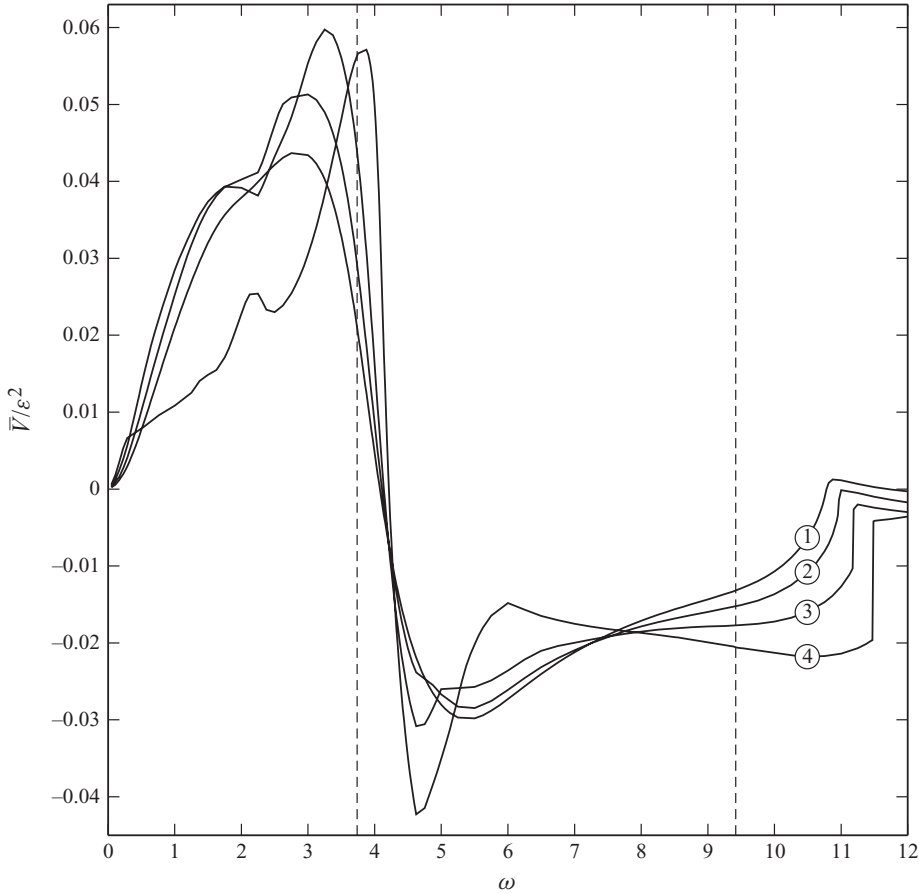


FIGURE 6. As in figures 4–5, but for the nonlinear contact-line law with hysteresis, (4.10), and $\varepsilon = 1$. (1) $\theta_r = \theta_a = 1$, (2) $\theta_r = 0.95$, $\theta_a = 1.05$; (3) $\theta_r = 0.875$, $\theta_a = 1.125$; (4) $\theta_r = 0.75$, $\theta_a = 1.25$. The real parts of the natural frequencies of the drop’s free oscillations are shown by vertical dashed lines.

two sloping downwards. This suggests that the drop favours upward motion at the expense of the downward one, and this asymmetry produces mean uphill drift.

5. Concluding remarks

In this paper, we have shown that the interaction of the substrate’s acceleration, inertia and surface tension is sufficient to explain the rise of a drop on a vibrating plate. We found that significant mean velocities can only occur away from the resonant frequencies of the drop, at least in a linear theory. The motion of the drop is controlled by the weakly nonlinear interaction of swaying and spreading (odd and even) modes, and this seems to be a fruitful way to think about the motion even when it becomes fully nonlinear. It is also shown that, in the absence of friction, drops slide down regardless of all other parameters.

Finally, we have not attempted to make a quantitative comparison between our simulations and the experiments of Brunet *et al.* (2007), since these experiments have $O(1)$ contact angles, and the shallow-water (thin-drop) approximation is not appropriate. We hope to address this case in a later paper, and also to extend our

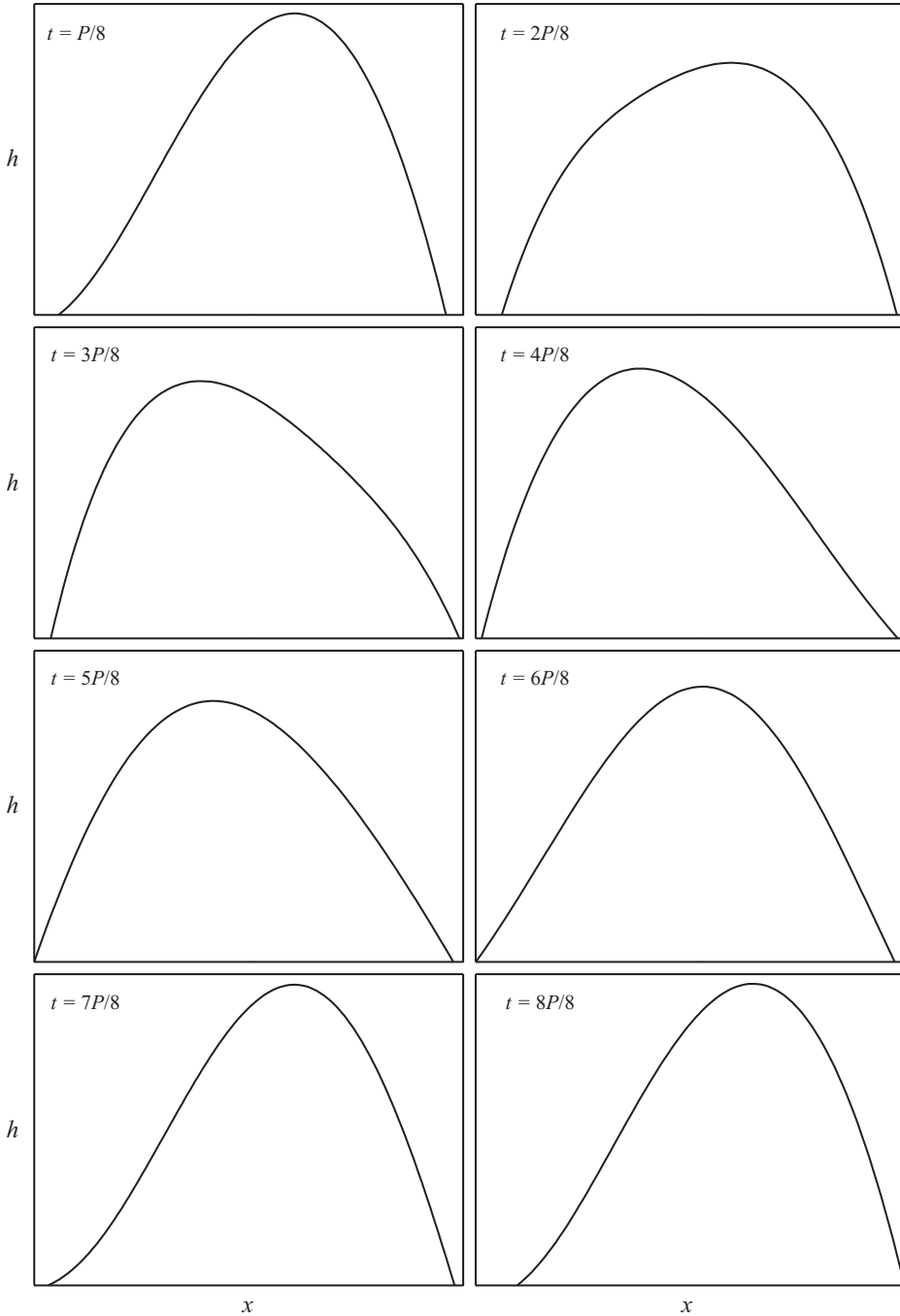


FIGURE 7. The shape of the drop, h versus x , through eight equally spaced times during one period P of the oscillation, as computed through simulations of the exact equations (3.7)–(3.10) for $g=0$, $\varepsilon=1$, $\gamma=5$, $\omega=4$, and the contact-line law (4.10) with $\theta_r=0.75$ and $\theta_a=1.25$.

results to three-dimensional drops, for which we expect that the more complex geometry of the contact line will have a significant quantitative, and possibly qualitative, effect on the dynamics. In the present work, we only target qualitative

agreement with the observed behaviour. We are also currently studying the dynamics of the drop when the boundary conditions require the contact angle to be constant, with a Navier-slip condition at the wall and sizable viscosity. This extension should provide us with more insight into the effect of viscosity on the drop; it can also capture the phenomenon of phase lag at the contact line observed experimentally by Brunet *et al.* (2007).

The authors are grateful to Professor John Hinch for pointing out the importance of separating the odd and even modes in the asymptotic analysis of the problem. They also acknowledge the support of the Science Foundation Ireland, delivered via RFP grant 08/RFP/MTH1476 and Mathematics Initiative grant 06/MI/005.)

Appendix A. The energy balance equation

In addition to the liquid–gas surface tension σ , we shall now introduce the solid–liquid tension σ_{sl} and the solid–gas tension σ_{sg} . Then, the total energy of the system can be written in the form

$$E = \int_{x_-}^{x_+} \left\{ \frac{1}{2} \rho h u^2 + \rho a \left(x \sin \alpha + \frac{1}{2} h \cos \alpha \right) h + \sigma \times \left[1 + \frac{1}{2} \left(\frac{\partial h}{\partial x} \right)^2 \right] + (\sigma_{sl} - \sigma_{sg}) \right\} dx, \quad (\text{A } 1)$$

where the first and second terms represent the kinetic and potential energies, the third term represents the surface energy of the liquid–gas interface derived in the thin-drop limit (the exact version would involve $\sqrt{1 + (\partial h / \partial x)^2}$ instead of $1 + (\partial h / \partial x)^2 / 2$), and the last term represents the energy difference associated with the replacement of the solid–gas interface by the solid–liquid one (and *vice versa*) when the drop expands (contracts).

The following energy balance equation can be derived from the governing equations (2.1)–(2.3):

$$\begin{aligned} \frac{dE}{dt} = & \frac{dx_+}{dt} \left\{ -\sigma \left(\frac{\partial h}{\partial x} \right)^2 + \sigma \left[1 + \frac{1}{2} \left(\frac{\partial h}{\partial x} \right)^2 \right] + (\sigma_{sl} - \sigma_{sg}) \right\}_{x=x_+} \\ & - \frac{dx_-}{dt} \left\{ -\sigma \left(\frac{\partial h}{\partial x} \right)^2 + \sigma \left[1 + \frac{1}{2} \left(\frac{\partial h}{\partial x} \right)^2 \right] + (\sigma_{sl} - \sigma_{sg}) \right\}_{x=x_-} \\ & + \frac{da}{dt} \int_{x_-}^{x_+} \rho \left(x \sin \alpha + \frac{1}{2} h \cos \alpha \right) h dx. \end{aligned} \quad (\text{A } 2)$$

The last term in (A 2) describes the potential energy change due to the oscillating gravity/inertial force (it is of no interest to us), whereas the first two terms describe the energy change at the contact lines.

Using the contact-line boundary condition (2.4), one can transform (A 2) into

$$\begin{aligned} \frac{dE}{dt} = & \frac{1}{2} \sigma \left[v(\theta_a) (\theta_0^2 - \theta_a^2) + v(\theta_r) (\theta_0^2 - \theta_r^2) \right] \\ & + \frac{da}{dt} \int_{x_-}^{x_+} \rho \left(x \sin \alpha + \frac{1}{2} h \cos \alpha \right) h dx, \end{aligned} \quad (\text{A } 3)$$

where

$$\theta_0 = \left[\frac{2(\sigma + \sigma_{sl} - \sigma_{sg})}{\sigma} \right]^{1/2}. \quad (\text{A } 4)$$

(Note that the above expression for θ_0 is the thin-film equivalent of the Laplace–Young formula for the equilibrium contact angle,

$$\cos \theta_0 = \frac{\sigma_{sg} - \sigma_{sl}}{\sigma}, \quad (\text{A } 5)$$

as the latter expression reduces to the former in the limit $\theta_0 \ll 1$.)

Most importantly, if $v(\theta)$ is as described by (2.5), and θ_0 lies within the hysteresis interval, the first term in (A 3) is negative – which means that energy is *dissipated* at the contact lines (whereas energy *generation* would render our model meaningless physically).

It is worth noting that, if we required the contact angles θ_{\pm} to always equal θ_0 ,

$$\left(\frac{\partial h}{\partial x} \right)_{x=x_{\pm}} = \mp \theta_0 \quad (\text{A } 6)$$

(which is an often used alternative to the boundary condition (2.4)), the first term in (A 2) would vanish. Physically, this means that the boundary condition (A 6) eliminates contact-line friction. Note also that the same result can be achieved by using our original boundary condition, (2.4), with, say,

$$v(\theta) = v'(\theta - \theta_0), \quad (\text{A } 7)$$

and taking the limit $v' \rightarrow \infty$.

Appendix B. The properties of, and a numerical method for, (3.21)–(3.23)

To examine the properties of the boundary-value problem (3.21)–(3.23), it is convenient to eliminate $h_1^{(1)}$ and replace $u_1^{(1)}$ with

$$\phi = u - \frac{1 - \gamma x}{\omega} + V, \quad (\text{B } 1)$$

where the subscripts 1 and superscripts (1) have both been omitted. In terms of ϕ , (3.21)–(3.23) have the form

$$\frac{1}{2\omega^2} \frac{d^4[\phi(1-x^2)]}{dx^4} - \phi = 0, \quad (\text{B } 2)$$

$$\phi \rightarrow V \pm \omega D - \frac{1 \mp \gamma}{\omega} \quad \text{as } x \rightarrow \pm 1, \quad (\text{B } 3)$$

$$(1-x^2) \frac{d\phi}{dx} \rightarrow 0 \quad \text{as } x \rightarrow \pm 1, \quad (\text{B } 4)$$

$$\mp \frac{1-x^2}{2} \frac{d^2\phi}{dx^2} + 2 \frac{d\phi}{dx} \rightarrow \frac{\omega(\omega D \pm V)}{iv'} + \frac{2\gamma}{\omega} \quad \text{as } x \rightarrow \pm 1. \quad (\text{B } 5)$$

Observe that the coefficient of the highest derivative of (B 2) vanishes as $x \rightarrow \pm 1$, which means that the boundary conditions (B 3)–(B 5) are set at singular points. Thus, to make sure that (B 3)–(B 5) are consistent with the (presumably singular) solutions, we should examine the behaviour of ϕ as $x \rightarrow \pm 1$.

It can be shown that the general solution of (B 2) can be represented in the form

$$\phi = \sum_{n=1}^4 C_n^- \phi_n^-, \quad (\text{B } 6)$$

where the particular solutions $\phi_{1,2,3,4}^-$ are fixed by their asymptotic behaviours as $x \rightarrow -1$,

$$\phi_1^- = \frac{1}{x+1} + O[(x+1)^2 \ln(x+1)] \quad \text{as } x \rightarrow -1, \quad (\text{B } 7)$$

$$\phi_2^- = 1 + O[(x+1)^3] \quad \text{as } x \rightarrow -1, \quad (\text{B } 8)$$

$$\phi_3^- = (x+1) + O[(x+1)^4] \quad \text{as } x \rightarrow -1, \quad (\text{B } 9)$$

$$\phi_4^- = \frac{(x+1)^2}{1-x} + O[(x+1)^5] \quad \text{as } x \rightarrow -1. \quad (\text{B } 10)$$

Substitution of (B 6) into the boundary condition (B 3)–(B 5) yields

$$C_1^- = 0, \quad C_2^- = V - \omega D - \frac{1+\gamma}{\omega}, \quad C_3^- = \frac{\omega(\omega D - V)}{2iv'} + \frac{\gamma}{\omega}, \quad (\text{B } 11)$$

whereas C_4^- remains undetermined.

Considering, in turn, the point $x = 1$, one can introduce another set of particular solutions of (B 2),

$$\phi_1^+ = \frac{1}{-x+1} + O[(-x+1)^2 \ln(-x+1)] \quad \text{as } x \rightarrow 1, \quad (\text{B } 12)$$

$$\phi_2^+ = 1 + O[(-x+1)^3] \quad \text{as } x \rightarrow 1, \quad (\text{B } 13)$$

$$\phi_3^+ = (-x+1) + O[(-x+1)^4] \quad \text{as } x \rightarrow 1, \quad (\text{B } 14)$$

$$\phi_4^+ = \frac{(-x+1)^2}{1+x} + O[(-x+1)^5] \quad \text{as } x \rightarrow 1, \quad (\text{B } 15)$$

and, thus, represent the solution of (B 2)–(B 5) by

$$\phi = \sum_{n=1}^4 C_n^+ \phi_n^+, \quad (\text{B } 16)$$

where

$$C_1^+ = 0, \quad C_2^+ = V + \omega D - \frac{1-\gamma}{\omega}, \quad C_3^+ = -\frac{\omega(\omega D + V)}{2iv'} - \frac{\gamma}{\omega} \quad (\text{B } 17)$$

and C_4^+ remains undetermined.

Given that (B 6)–(B 11) and (B 16)–(B 17) represent the same solution, we require that they coincide at an intermediate point, say x_0 , i.e.

$$\sum_{n=1}^4 C_n^- \phi_n^- = \sum_{n=1}^4 C_n^+ \phi_n^+ \quad \text{at } x = x_0, \quad (\text{B } 18)$$

$$\sum_{n=1}^4 C_n^- \frac{d\phi_n^-}{dx} = \sum_{n=1}^4 C_n^+ \frac{d\phi_n^+}{dx} \quad \text{at } x = x_0, \quad (\text{B } 19)$$

$$\sum_{n=1}^4 C_n^- \frac{d^2\phi_n^-}{dx^2} = \sum_{n=1}^4 C_n^+ \frac{d^2\phi_n^+}{dx^2} \quad \text{at } x = x_0, \quad (\text{B } 20)$$

$$\sum_{n=1}^4 C_n^- \frac{d^3 \phi_n^-}{dx^3} = \sum_{n=1}^4 C_n^- \frac{d^3 \phi_n^+}{dx^3} \quad \text{at } x = x_0. \quad (\text{B } 21)$$

Upon substitution of (B 11), (B 17) into (B 18)–(B 21), the latter set should be viewed as equations for V , D , C_4^- and C_4^+ . Given that the number of the equations matches the number of the unknowns, we conclude that the boundary-value problem (B 2)–(B 5) is a consistent one.

Equations (B 18)–(B 21), (B 11), (B 17) also provide a means for solving the boundary-value problem (B 2)–(B 5) numerically. Computing ϕ_n^\pm by ‘shooting’ the solution from $x = \pm 1$ towards an intermediate point x_0 , one can calculate the coefficients of the (linear) set (B 18)–(B 21) and solve it. Having found V , D , and C_4^\pm , one can use (B 6)–(B 11) and (B 16)–(B 17) to compute the solution in the intervals $(-1, x_0)$ and $(x_0, 1)$ respectively.

Appendix C. Asymptotic solutions of (3.21)–(3.23)

C.1. The small- ω limit

Omitting (as in Appendix B) the superscript (1) and assuming $|\omega| \ll 1$, we seek a solution in the form

$$h = h_{(0)} + \omega h_{(1)} + \dots, \quad u = \omega u_{(1)} + \dots, \quad (\text{C } 1)$$

$$D = D_{(0)} + \omega D_{(1)} + \dots, \quad V = V_{(0)} + \omega V_{(1)} + \dots. \quad (\text{C } 2)$$

To leading order, (3.21)–(3.23) yield

$$\frac{d^3 h_{(0)}}{dx^3} = 1 - \gamma x, \quad (\text{C } 3)$$

$$h_{(0)} + \frac{1}{2} \frac{d[u_{(1)}(1-x^2)]}{dx} = 0, \quad (\text{C } 4)$$

$$h_{(0)} = D_{(0)}, \quad u_{(1)} = \pm D_{(0)} \quad \text{at } x = \pm 1, \quad (\text{C } 5)$$

$$\frac{dh_{(0)}}{dx} = \frac{1}{iv'} V_{(0)} \pm D_{(0)} \quad \text{at } x = \pm 1. \quad (\text{C } 6)$$

This boundary-value problem can readily be solved:

$$h_{(0)} = \frac{x^3}{6} - \frac{\gamma x^4}{24} + \frac{\gamma x^2}{10} - \frac{x}{6} - \frac{\gamma}{40}, \quad u_{(1)} = -\frac{\gamma x(x^2-3)}{60} + \frac{x^2-1}{12}, \quad (\text{C } 7)$$

$$V_{(0)} = \frac{iv'}{3}, \quad D_{(0)} = \frac{\gamma}{30}. \quad (\text{C } 8)$$

To the next-to-leading order, (3.21)–(3.23) yield

$$V_{(0)} + \frac{d^3 h_{(1)}}{dx^3} = 0, \quad (\text{C } 9)$$

$$h_{(1)} + \frac{1}{2} \frac{d[u_{(2)}(1-x^2)]}{dx} = 0, \quad (\text{C } 10)$$

$$h_{(1)} = D_{(1)}, \quad u_{(2)} = \pm D_{(1)} \quad \text{at } x = \pm 1, \quad (\text{C } 11)$$

$$\frac{dh_{(1)}}{dx} = \frac{1}{iv'} (V_{(1)} \pm D_{(0)}) \pm D_{(1)} \quad \text{at } x = \pm 1. \quad (\text{C } 12)$$

The solution for $h_{(1)}$ and $u_{(2)}$ will not be presented here as we only need

$$V_{(1)} = \frac{(v')^2}{9}, \quad D_{(1)} = -\frac{\gamma i}{60v'}. \quad (\text{C } 13)$$

Now, substituting (C 8)–(C 13) into expression (3.44) for \bar{V} and assuming $g \sim \omega^2$, we obtain

$$\bar{V} \approx \varepsilon^2 \left\{ \frac{\gamma}{360v'} \left(1 - \frac{v''}{v'} \right) \left[1 - \frac{2(v')^2}{3} \right] \omega^2 - \frac{v'g}{2} \right\} \quad \text{as } \omega \rightarrow 0. \quad (\text{C } 14)$$

C.2. The large- ω limit

In what follows, we shall use the variable $\Phi = (1 - x^2)\phi$ and represent the solution by a sum of the odd and even parts, $\Phi = \Phi_e + \Phi_o$, with

$$\frac{d^4 \Phi_e}{dx^4} - \frac{2\omega^2}{1 - x^2} \Phi_e = 0, \quad (\text{C } 15)$$

$$\left. \begin{aligned} \Phi_e &= 0, \\ \frac{d\Phi_e}{dx} &= \pm 2 \left(\frac{1}{\omega} - V \right), \\ \frac{d^2 \Phi_e}{dx^2} &= 2 \left[\frac{1}{\omega} - \left(\frac{\omega}{iv'} + 1 \right) V \right], \end{aligned} \right\} \quad \text{at } x = \pm 1, \quad (\text{C } 16)$$

$$\frac{d^4 \Phi_o}{dx^4} - \frac{2\omega^2}{1 - x^2} \Phi_o = 0, \quad (\text{C } 17)$$

$$\left. \begin{aligned} \Phi_o &= 0, \\ \frac{d\Phi_o}{dx} &= -2 \left(\frac{\gamma}{\omega} + \omega D \right), \\ \frac{d^2 \Phi_o}{dx^2} &= \mp 2 \left[\frac{3\gamma}{\omega} + \left(\frac{\omega}{iv'} + 1 \right) \omega D \right], \end{aligned} \right\} \quad \text{at } x = \pm 1 \quad (\text{C } 18)$$

(as before, the superscript (1) has been omitted here). Using the standard WKBJ substitution, $\Phi = \exp(\omega^{1/2}\Psi)$, we can show that, in the limit $\omega \rightarrow \infty$,

$$\Phi_e \sim (1 - x^2)^{3/8} [c_1 \cos \omega^{1/2} f(x) + c_2 \cosh \omega^{1/2} f(x)], \quad (\text{C } 19)$$

$$\Phi_o \sim (1 - x^2)^{3/8} [c_3 \sin \omega^{1/2} f(x) + c_4 \sinh \omega^{1/2} f(x)], \quad (\text{C } 20)$$

where

$$f(x) = 2^{1/4} \int_0^x (1 - s^2)^{-1/4} ds. \quad (\text{C } 21)$$

The presence of singularities in (C 15) and (C 17) at $x = \pm 1$ indicates that the boundary conditions (C 16) and (C 18) can be satisfied only if boundary layers are introduced at these points, with widths of $O(\omega^{-2/3})$. Due to the symmetry of the problem, it is sufficient to consider the layer at $x = 1$.

We now define an inner variable, $X = \omega^{2/3} (1 - x)$. Formally, we should also re-scale V , D , Φ_e and Φ_o , but – since this is a linear problem – the algebra is clearer if we do not do this. Re-scaling (C 15)–(C 18) and keeping the leading-order terms only, we obtain

$$\frac{d^4 \Phi_e}{dX^4} - \frac{1}{X} \Phi_e = 0, \quad (\text{C } 22)$$

$$\left. \begin{aligned} \Phi_e &= 0, \\ \frac{d\Phi_e}{dX} &= -2\omega^{-2/3} \left(\frac{1}{\omega} - V \right), \\ \frac{d^2\Phi_e}{dx^2} &= 2\omega^{-4/3} \left[\frac{1}{\omega} - \left(\frac{\omega}{iv'} + 1 \right) V \right], \end{aligned} \right\} \text{ as } X \rightarrow 0, \quad (\text{C 23})$$

$$\frac{d^4\Phi_o}{dX^4} - \frac{1}{X}\Phi_o = 0, \quad (\text{C 24})$$

$$\left. \begin{aligned} \Phi_o &= 0, \\ \frac{d\Phi_o}{dX} &= -2\omega^{-2/3} \left(\frac{\gamma}{\omega} + \omega D \right), \\ \frac{d^2\Phi_o}{dx^2} &= -2\omega^{-4/3} \left[\frac{3\gamma}{\omega} + \left(\frac{\omega}{iv'} + 1 \right) \omega D \right], \end{aligned} \right\} \text{ as } X \rightarrow 0. \quad (\text{C 25})$$

To match the boundary-layer solution to the outer solution (C 19)–(C 20), rewrite the latter in terms of X and consider the limit $X \rightarrow \infty$, which yields

$$\begin{aligned} \Phi_e &\sim 2^{-5/8}\omega^{-1/3}X^{3/8} \left\{ c_1 [\exp(i\omega^{1/2}f(1) - \frac{4}{3}iX^{3/4}) + \exp(-i\omega^{1/2}f(1) + \frac{4}{3}iX^{3/4})] \right. \\ &\quad \left. + c_2 [\exp(\omega^{1/2}f(1) - \frac{4}{3}X^{3/4}) + \exp(-\omega^{1/2}f(1) + \frac{4}{3}X^{3/4})] \right\} \text{ as } X \rightarrow \infty, \quad (\text{C 26}) \end{aligned}$$

$$\begin{aligned} \Phi_o &\sim 2^{-5/8}\omega^{-1/3}X^{3/8} \left\{ -ic_3 [\exp(i\omega^{1/2}f(1) - \frac{4}{3}iX^{3/4}) - \exp(i\omega^{1/2}f(1) + \frac{4}{3}iX^{3/4})] \right. \\ &\quad \left. + c_4 [\exp(\omega^{1/2}f(1) - \frac{4}{3}X^{3/4}) - \exp(-\omega^{1/2}f(1) + \frac{4}{3}X^{3/4})] \right\} \text{ as } X \rightarrow \infty, \quad (\text{C 27}) \end{aligned}$$

where

$$f(1) = 2^{1/4} \int_0^1 (1-s^2)^{-1/4} ds = \frac{2^{5/4} \sqrt{\pi} \Gamma(\frac{3}{4})}{\Gamma(\frac{1}{4})} \approx 1.43. \quad (\text{C 28})$$

The inner solution $\Phi_{e,o}$ is fully determined by (C 22)–(C 27).

At first sight, it seems we should be able to solve (C 22) and (C 24) using Mellin integral transforms (see King 1991) – but, since the solutions grow exponentially as $X \rightarrow \infty$, this is not the case. Instead, we recall from Appendix B that four linearly independent solutions can be defined through

$$\Phi_1 \sim 1, \quad \Phi_2 \sim X, \quad \Phi_3 \sim X^2, \quad \Phi_4 \sim X^3 \text{ as } X \rightarrow 0. \quad (\text{C 29})$$

As $X \rightarrow \infty$, a straightforward analysis of (C 22) and (C 24) shows that $\Phi_{1,2,3,4}$ should be linear combinations of $X^{3/8} e^{\pm 4iX^{3/4}/3}$, $X^{3/8} e^{\pm 4iX^{3/4}/3}$ – i.e.

$$\begin{bmatrix} \Phi_1 \\ \Phi_2 \\ \Phi_3 \\ \Phi_4 \end{bmatrix} \sim \begin{bmatrix} A_{11} & A_{12} & A_{13} & A_{14} \\ A_{21} & A_{22} & A_{23} & A_{24} \\ A_{31} & A_{32} & A_{33} & A_{34} \\ A_{41} & A_{42} & A_{43} & A_{44} \end{bmatrix} \begin{bmatrix} X^{3/8} e^{-4iX^{3/4}/3} \\ X^{3/8} e^{4iX^{3/4}/3} \\ X^{3/8} e^{-4iX^{3/4}/3} \\ X^{3/8} e^{4iX^{3/4}/3} \end{bmatrix} \text{ as } X \rightarrow \infty, \quad (\text{C 30})$$

where A_{nm} are undetermined constants. Note also that the coefficients of (C 22) and (C 24) are real, and so should be $\Phi_{1,2,3,4}$ – hence,

$$A_{n,2} = A_{n,1}^*, \quad \text{Im } A_{n,3} = 0, \quad \text{Im } A_{n,4} = 0. \quad (\text{C 31})$$

Observe that, since ω does not appear in (C 22) and (C 24), $A_{nm} = O(1)$ as $\omega \rightarrow \infty$, and this is all that we need to make progress.

It follows from the boundary conditions (C 23) and (C 25) that

$$\Phi_e = -2\omega^{-2/3} \left(\frac{1}{\omega} - V \right) \Phi_2 + \omega^{-4/3} \left[\frac{1}{\omega} - \left(\frac{\omega}{iv'} + 1 \right) V \right] \Phi_3 + B_e \Phi_4, \quad (\text{C } 32)$$

$$\Phi_o = -2\omega^{-2/3} \left(\frac{\gamma}{\omega} + \omega D \right) \Phi_2 - \omega^{-4/3} \left[\frac{3\gamma}{\omega} + \left(\frac{\omega}{iv'} + 1 \right) \omega D \right] \Phi_3 + B_o \Phi_4, \quad (\text{C } 33)$$

where B_e and B_o are constants to be determined.

We are interested in how the solution of the full (forced) problem behaves when ω equals one of the eigenvalues of the unforced problem – thus, let us consider the latter. For the odd mode, from (C 26) we can determine the four equations that connect c_1 , c_2 , V , B_e and ω

$$2^{-5/8} \omega^{-1/4} e^{i\omega^{1/2} f(1)} c_1 = -\frac{\omega^{-1/3}}{iv'} V A_{31} + B_e A_{41}, \quad (\text{C } 34)$$

$$2^{-5/8} \omega^{-1/4} e^{-i\omega^{1/2} f(1)} c_1 = -\frac{\omega^{-1/3}}{iv'} V A_{31}^* + B_e A_{41}^*, \quad (\text{C } 35)$$

$$2^{-5/8} \omega^{-1/4} e^{-\omega^{1/2} f(1)} c_2 = -\frac{\omega^{-1/3}}{iv'} V A_{33} + B_e A_{43}, \quad (\text{C } 36)$$

$$0 = -\frac{\omega^{-1/3}}{iv'} V A_{34} + B_e A_{43}. \quad (\text{C } 37)$$

Eliminating c_1 , c_2 , B_e and V , we find that

$$e^{2i\omega^{1/2} f(1)} = \frac{A_{41} A_{34} - A_{31} A_{43}}{A_{41}^* A_{34} - A_{31}^* A_{43}}. \quad (\text{C } 38)$$

The right-hand side is a complex number with unit modulus, and therefore ω is real at leading order, and

$$\omega^{1/2} \sim \Omega_0 + n\Omega_1, \quad (\text{C } 39)$$

where Ω_0 is an undetermined real constant, and

$$\Omega_1 = \frac{\pi}{f(1)} \approx 2.20. \quad (\text{C } 40)$$

Note that, when we repeat this analysis for the odd modes, we again obtain (C 34)–(C 37), but with plus on the right-hand side. This means that the odd modes are also given by (C 39)–(C 40), but with $\omega^{1/2}$ shifted by $\Omega_1/2$, so that the odd and even modes are interleaved and, for $\omega \gg 1$, equally spaced.

Our numerical results suggest that (C 39)–(C 40) describe the spacing of the natural frequencies well, and even for moderate values of ω . For the first two odd modes, for example, we have

$$\omega_{o2} - \omega_{o1} \approx 2.25 - 0.12i, \quad (\text{C } 41)$$

whereas figure 3 illustrates that the spacing of $(\text{Re } \omega)^{1/2}$ is indeed close to uniform. Figure 8, in turn, shows the real and imaginary parts of the natural frequencies, suggesting that the imaginary part is $O(\omega^{1/6})$ (with a coefficient of 0.835 providing the best fit). Establishing this from our asymptotic analysis requires calculation of the correction term in the expansions, and we have not pursued this further.

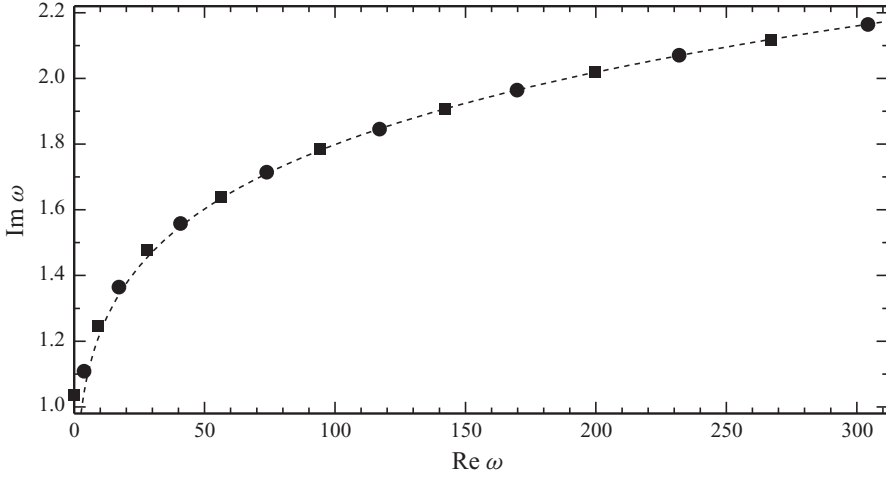


FIGURE 8. The real and imaginary parts of the natural frequencies of the drop's free oscillations. The squares/circles show even/odd modes. The dashed line shows the dependence $\text{Im } \omega = 0.835 (\text{Re } \omega)^{1/6}$.

In the forced problem, we find that

$$2^{-5/8} \omega^{-1/4} e^{i\omega^{1/2} f(1)} c_1 \sim -2\omega^{-2/3} \left(\frac{1}{\omega} - V \right) A_{21} - \frac{\omega^{-1/3}}{i v'} V A_{31} + B_e A_{41}, \quad (\text{C } 42)$$

$$2^{-5/8} \omega^{-1/4} e^{-i\omega^{1/2} f(1)} c_1 \sim -2\omega^{-2/3} \left(\frac{1}{\omega} - V \right) A_{21}^* - \frac{\omega^{-1/3}}{i v'} V A_{31}^* + B_e A_{41}^*, \quad (\text{C } 43)$$

$$2^{-5/8} \omega^{-1/4} e^{-\omega^{1/2} f(1)} c_2 \sim -2\omega^{-2/3} \left(\frac{1}{\omega} - V \right) A_{23} - \frac{\omega^{-1/3}}{i v'} V A_{33} + B_e A_{43}, \quad (\text{C } 44)$$

$$0 \sim -2\omega^{-2/3} \left(\frac{1}{\omega} - V \right) A_{24} - \frac{\omega^{-1/3}}{i v'} V A_{34} + B_e A_{43}. \quad (\text{C } 45)$$

At the resonant frequencies, these equations are simply (C 34)–(C 37), with the addition of the terms involving $(1/\omega - V)$ – so the obvious solution is $V = 1/\omega$ (as confirmed by figure 3). A similar analysis of the leading-order equations for the odd mode at the resonant frequency for the even mode shows that $D \sim i C_1 v' \gamma \omega^{-7/3}$, where C_1 is a real constant that we can determine in terms of A_{ij} , v' and ω . The analysis at the odd resonant frequencies is much the same and shows that $D \sim -\gamma/\omega^2$ and $V \sim i C_2 v' \omega^{-4/3}$, with C_2 a real constant that we can determine in terms of A_{ij} , v' and ω . In each case, we conclude that, at the resonant frequencies, D and V are $\pi/2$ out of phase with each other, consistent with our numerical results.

Away from the resonant frequencies, a balancing of terms in (C 45) shows that $V = O(\omega^{-4/3})$, and the leading-order solution has $V \sim i C_3 \omega^{-4/3}$. Similarly $D \sim i C_4 \omega^{-7/3}$, where C_3 and C_4 are real constants that we can determine in terms of A_{ij} , v' and ω .

Appendix D. The second-order calculations

At $O(\varepsilon^2)$, the governing equations (3.7)–(3.10) yield

$$\frac{\partial u^{(2)}}{\partial t} + \frac{dV^{(2)}}{dt} + u^{(1)} \frac{\partial u^{(1)}}{\partial x} - \frac{\partial^3 h^{(2)}}{\partial x^3} = -\gamma \sin \omega t \frac{\partial h^{(1)}}{\partial x} - g \left(1 + \gamma \frac{\partial h^{(0)}}{\partial x} \right), \quad (\text{D } 1)$$

$$\frac{\partial h^{(2)}}{\partial t} + \frac{\partial (u^{(1)}h^{(1)} + u^{(2)}h^{(0)})}{\partial x} = 0, \quad (\text{D } 2)$$

$$h^{(2)} \pm \frac{\partial h^{(0)}}{\partial x} D^{(2)} \pm \frac{\partial h^{(1)}}{\partial x} D^{(1)} + \frac{1}{2} \frac{\partial^2 h^{(0)}}{\partial x^2} (D^{(1)})^2 = 0 \quad \text{at } x = \pm D^{(0)}, \quad (\text{D } 3)$$

$$u^{(2)} \pm \frac{\partial u^{(1)}}{\partial x} D^{(1)} = \pm \frac{dD^{(2)}}{dt} \quad \text{at } x = \pm D^{(0)}, \quad (\text{D } 4)$$

$$V^{(2)} \pm \frac{dD^{(2)}}{dt} = -v' \left[\frac{\partial h^{(2)}}{\partial x} \pm \frac{\partial^2 h^{(0)}}{\partial x^2} D^{(2)} \pm \frac{\partial^2 h^{(1)}}{\partial x^2} D^{(1)} + \frac{1}{2} \frac{\partial^3 h^{(0)}}{\partial x^3} (D^{(1)})^2 \right]_{x=\pm D^{(0)}} \\ \pm \frac{v''}{2} \left[\left(\frac{\partial h^{(1)}}{\partial x} \pm \frac{\partial^2 h^{(0)}}{\partial x^2} D^{(1)} \right)_{x=\pm D^{(0)}} \right]^2. \quad (\text{D } 5)$$

We shall seek a solution of the form

$$u^{(2)}(x, t) = u_0^{(2)}(x) + \text{Re} [u_2^{(2)}(x) e^{2i\omega t}], \quad h^{(2)}(x, t) = h_0^{(2)}(x) + \text{Im} [h_2^{(2)}(x) e^{2i\omega t}], \quad (\text{D } 6)$$

$$V^{(2)}(t) = V_0^{(2)} + \text{Re} [V_2^{(2)} e^{2i\omega t}], \quad D^{(2)}(t) = D_0^{(2)} + \text{Im} [\hat{D}_2^{(2)} e^{2i\omega t}]. \quad (\text{D } 7)$$

Substituting these expressions into (D 1)–(D 5), one can obtain two separate sets of equations for $(u_0^{(2)}, h_0^{(2)}, V_0^{(2)}, D_0^{(2)})$ and $(u_2^{(2)}, h_2^{(2)}, V_2^{(2)}, D_2^{(2)})$. In what follows, we only need the boundary-value problem for $h_0^{(2)}$, so the rest of the equations/boundary conditions will not be presented,

$$\frac{d^3 h_0^{(2)}}{dx^3} = \frac{1}{4} \left(u_1^{(1)} \frac{du_1^{(1)*}}{dx} + u_1^{(1)*} \frac{du_1^{(1)}}{dx} \right) + \frac{\gamma}{4} \left(\frac{dh_1^{(1)}}{dx} + \frac{dh_1^{(1)*}}{dx} \right) + g \left(1 + \gamma \frac{dh^{(0)}}{dx} \right), \quad (\text{D } 8)$$

$$h_0^{(2)} = \mp \frac{dh^{(0)}}{dx} D_0^{(2)} \mp \frac{1}{4} \left(\frac{dh_1^{(1)}}{dx} D_1^{(1)*} + \frac{dh_1^{(1)*}}{dx} D_1^{(1)} \right) \\ - \frac{1}{4} \frac{d^2 h^{(0)}}{dx^2} \left| D_1^{(1)} \right|^2 \quad \text{at } x = \pm D^{(0)}, \quad (\text{D } 9)$$

$$\frac{dh_0^{(2)}}{dx} = \mp \frac{d^2 h^{(0)}}{dx^2} D_0^{(2)} \mp \frac{1}{4} \left(\frac{d^2 h_1^{(1)}}{dx^2} D_1^{(1)*} + \frac{d^2 h_1^{(1)*}}{dx^2} D_1^{(1)} \right) - \frac{1}{4} \frac{d^3 h^{(0)}}{dx^3} \left| D_1^{(1)} \right|^2 - \frac{1}{v'} V_0^{(2)} \\ \pm \frac{v''}{4v'} \left| \frac{dh_1^{(1)}}{dx} \pm \frac{d^2 h^{(0)}}{dx^2} D_1^{(1)} \right|^2 \quad \text{at } x = \pm D^{(0)}. \quad (\text{D } 10)$$

Next we integrate (D 9),

$$\frac{d^2 h_0^{(2)}}{dx^2} = \frac{1}{4} \left| u_1^{(1)} \right|^2 + \frac{\gamma}{4} (h_1^{(1)} + h_1^{(1)*}) + g(x + \gamma h^{(0)}) + \text{const}, \quad (\text{D } 11)$$

and then multiply the resulting equation by x and integrate again, this time from $x = -D^{(0)}$ to $x = D^{(0)}$. Taking into account the boundary conditions (D 9)–(D 10) and

recalling expression (3.14) for $h^{(0)}$, we obtain

$$\begin{aligned}
& -\frac{2}{v'} V_0^{(2)} + \frac{v''}{4v'} \left[\left(\left| \frac{dh_1^{(1)}}{dx} - D_1^{(1)} \right|^2 \right)_{x=1} - \left(\left| \frac{dh_1^{(1)}}{dx} + D_1^{(1)} \right|^2 \right)_{x=-1} \right] \\
& - \frac{1}{2} \operatorname{Re} \left\{ \left[\left(\frac{d^2 h_1^{(1)}}{dx^2} \right)_{x=1} - \left(\frac{d^2 h_1^{(1)}}{dx^2} \right)_{x=-1} \right] D_1^{(1)*} \right\} \\
& + \frac{1}{2} \operatorname{Re} \left[\left(\frac{dh_1^{(1)}}{dx} \right)_{x=1} D_1^{(1)*} + \left(\frac{dh_1^{(1)}}{dx} \right)_{x=-1} D_1^{(1)*} \right] \\
& = \int_{-1}^1 \left(\frac{1}{4} |u_1^{(1)}|^2 + \frac{\gamma}{2} \operatorname{Re} h_1^{(1)} \right) x \, dx + g. \tag{D 12}
\end{aligned}$$

This equation can be simplified using the boundary conditions (3.17) for $h^{(1)}$,

$$\begin{aligned}
V_0^{(2)} &= -\frac{g v'}{2} - \frac{v'}{4} \int_{-1}^1 \left(\frac{1}{2} |u_1^{(1)}|^2 + \gamma \operatorname{Re} h_1^{(1)} \right) x \, dx \\
& - \frac{v'}{4} \operatorname{Re} \left\{ \left[\left(\frac{d^2 h_1^{(1)}}{dx^2} \right)_{x=1} - \left(\frac{d^2 h_1^{(1)}}{dx^2} \right)_{x=-1} \right] D_1^{(1)*} \right\} \\
& + \frac{1}{2} \operatorname{Im} (V_1^{(1)} D_1^{(1)*}) + \frac{\omega v''}{2(v')^2} \operatorname{Re} (V_1^{(1)} D_1^{(1)*}). \tag{D 13}
\end{aligned}$$

This is the desired expression for the drop's mean velocity. It looks different (more complicated), however, than its counterpart, (3.32), resulting from the momentum balance – and, to show the equivalence of the two, one needs to extensively use the properties of the first-order problem.

Firstly, observe that, as follows from the second equation of the set (3.21),

$$\int_{-1}^1 h_1^{(1)} \, dx = 0. \tag{D 14}$$

Secondly, multiply the first equation of the set (3.21) by $h_1^{(1)*}$, integrate it from $x = -1$ to $x = 1$, and take the real part, which yields

$$\begin{aligned}
\omega \int_{-1}^1 (u_1^{(1)} h_1^{(1)*} + u_1^{(1)*} h_1^{(1)}) \, dx + \int_{-1}^1 \left(\frac{d^3 h_1^{(1)}}{dx^3} h_1^{(1)*} + \frac{d^3 h_1^{(1)*}}{dx^3} h_1^{(1)} \right) \, dx \\
= -\gamma \int_{-1}^1 (h_1^{(1)*} + h_1^{(1)}) x \, dx. \tag{D 15}
\end{aligned}$$

A similar manipulation with the second equation of the set (3.21) yields

$$\begin{aligned}
\omega \int_{-1}^1 (h_1^{(1)} u_1^{(1)*} + h_1^{(1)*} u_1^{(1)}) \, dx \\
+ \frac{1}{2} \int_{-1}^1 \left\{ \frac{d[u_1^{(1)}(1-x^2)]}{dx} u_1^{(1)*} + \frac{d[u_1^{(1)*}(1-x^2)]}{dx} u_1^{(1)} \right\} \, dx = 0. \tag{D 16}
\end{aligned}$$

Subtracting (D 15) from (D 16), integrating by parts the integrals involving the third derivatives of $h_1^{(1)}$ and $h_1^{(1)*}$, and taking into account the boundary conditions (3.22)–

(3.23) and identity (D 14), one can obtain (after long cumbersome algebra)

$$\operatorname{Re} \left\{ \left[\left(\frac{d^2 h_1^{(1)}}{dx^2} \right)_{x=1} - \left(\frac{d^2 h_1^{(1)}}{dx^2} \right)_{x=-1} \right] D_1^{(1)*} \right\} + \int_{-1}^1 \left(\frac{1}{2} |u_1^{(1)}|^2 + \gamma \operatorname{Re} h \right) x \, dx - \frac{2}{v'} \operatorname{Im} \left(V_1^{(1)} D_1^{(1)*} \right) - \frac{2\omega}{(v')^2} \operatorname{Re} \left(V_1^{(1)} D_1^{(1)*} \right) = 0. \quad (\text{D } 17)$$

Using this identity, one can reduce (D 13) to expression (3.44) resulting from the momentum balance.

REFERENCES

- BENILOV, E. S. 2010 Drops climbing uphill on a slowly oscillating substrate. *Phys. Rev. E* **82**, 026320.
- BRUNET, P., EGGERS, J. & DEEGAN, R. D. 2007 Vibration-induced climbing of drops. *Phys. Rev. Lett.* **99**, 144501.
- BRUNET, P., EGGERS, J. & DEEGAN, R. D. 2009 Motion of a drop driven by substrate vibrations. *Eur. Phys. J. Special Topics* **166**, 11–14.
- CENICEROS, H. D. & HOU, T. Y. 1998 Convergence of a non-stiff boundary integral method for interfacial flows with surface tension. *Math. Comput.* **67**, 137–182.
- DANIEL, S., CHAUDHURY, M. K. & DE GENNES, P.-G. 2005 Vibration-actuated drop motion on surfaces for batch microfluidic processes. *Langmuir* **21**, 4240–4248.
- DAVIS, S. H. 2002 Interfacial fluid dynamics. In *Perspectives in Fluid Dynamics: A Collective Introduction to Current Research* (ed. G. K. Batchelor, H. K. Moffatt & M. G. Worster), pp. 1–51. Cambridge University Press.
- DOLD, J. W. 1992 An efficient surface-integral algorithm applied to unsteady gravity waves. *J. Comput. Phys.* **103**, 90–115.
- HOCKING, L. M. 1987 The damping of capillary gravity-waves at a rigid boundary. *J. Fluid Mech.* **179**, 253–266.
- HOCKING, L. M. & DAVIS, S. H. 2002 Inertial effects in time-dependent motion of thin films and drops. *J. Fluid Mech.* **467**, 1–17.
- KING, A. C. 1991 Moving contact lines in slender fluid wedges. *Q. J. Mech. Appl. Maths* **44**, 173–192.
- NOBLIN, X., KOFMAN, R. & CELESTINI, F. 2009 Ratchetlike motion of a shaken drop. *Phys. Rev. Lett.* **102**, 194504.